THE BALTIC JOURNAL
OF ROAD AND BRIDGE ENGINEERING

ISSN 1822-427X / eISSN 1822-4288
2016 Volume 11(1): 1–10

MODELLING OF JOINING ROUTE SEGMENTS OF DIFFERENT CURVATURE

Władysław Koc[1]✉, Katarzyna Palikowska[2]

Dept of Civil and Environmental Engineering, Gdansk University of Technology, 80–233 Gdansk, Poland
E-mails: [1] kocwl@pg.gda.pl; [2] katpalik@pg.gda.pl

Abstract. The paper presents a new general method of modelling route segments curvature using differential equations. The method enables joining of route segments of different curvature. Transitional curves of linear and nonlinear curvatures have been identified in the case of joining two circular arcs by *S*-shaped and *C*-oval transitions. The obtained *S*-shaped curves have been compared to the cubic *C*-Bezier curves and to the Pythagorean hodograph quantic Bezier curve using the Lateral Change of Acceleration diagram and the dynamic model. The analysis of dynamic properties has showed an advantage of the obtained transition curve of nonlinear curvature over Bezier curves.

Keywords: curvature, Bezier curve, differential equations, dynamic analysis, highway, lateral change of acceleration, transition curve.

1. Introduction

The issue of geometrical layout design of the transport routes has a very long history. Initially, the existing options have been very limited due to the level of both, computer technology and geodetic methods of setting out the routes. Therefore, numerous simplifications and approximate methods have been widely used. The revolution in the field of computer technology, which occurred at the end of the twentieth century, did not result in an immediate improvement in the design of geometrical layout of transport routes. Most of the traditional algorithms are still being used without any changes and their simplifying assumptions have not been replaced by more accurate ones.

In many cases the development of commercial Computer-Aided Design (CAD) applications is characterized by an excessive form of expansion which is not accompanied by the substantial content improvement. To solve this, it is necessary to carry on a development of the new computational algorithms taking into account the current state-of-the-art, which will inspire further research (Koc, Chrostowski 2013). Of particular importance here is the problem of vehicle dynamics, and, therefore, the proper modelling of curvature becomes crucial (Baykal 1996; Koc, Palikowska 2012; Li *et al.* 2010; Long *et al.* 2010).

The development of a method for precise determination of route coordinates seems to be the most appropriate course of action (Ahmad, Ali 2008; Bosurgi, D'Andrea 2012; Bosurgi *et al.* 2016; Kobryń 2011, 2014; Koc 2014; Ziatdinov *et al.* 2012a, 2012b). This paper provides the examples of such an approach, which radically diverges from the traditional approach. The analytical solutions, the most favourable in practical use, are obtained using the method described in the paper.

2. Joining two route segments

The examination of elementary geometrical situation is used to introduce the basic facts and notations. The example, presented in Fig. 1, shows two horizontal curves K_1 and K_2, away from one another, have their relative position clearly defined; curve K_1 has its endpoint curvature k_1 and the curve K_2 is at its point of origin, the curvature k_2. A system of coordinates x, y with its point of origin O is created in a way to make the point O to be the tangential point of curve K_1 and the x axis (Fig. 1).

Coordination systems of both curves, K_1 and K_2 (system x_1, y_1 and system x_2, y_2 respectively) are simultaneously transformed to the same system of coordinates x, y.

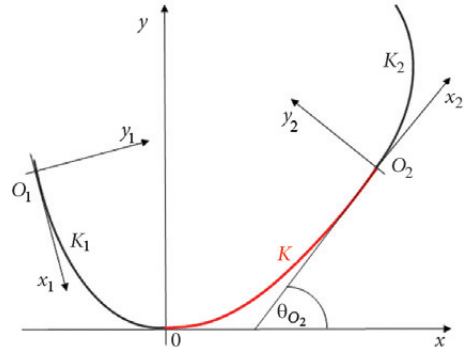

Fig. 1. Schema of the geometrical route layout

doi:10.3846/bjrbe.2016.01

The coordinates (x_{O_2}, y_{O_2}) of the point O_2, the position of the origin point of a curve K_2 and the value of the angle of a tangent θ at that point are obtained.

The main task consists of inscribing the transition curve $y(x)$ which joins the points O and O_2 and fulfils the boundary conditions. As it is shown in the literature (Koc, Mieloszyk 1998), the differential equations method has been applied to solve this task analytically. The differential equations method has evolved as a result of the generalization of lateral unbalanced acceleration identification regarding to transition curves (Mieloszyk, Koc 1991).

Thus, the transition curve in an explicit form that has been searched among the solutions of the following differential equation:

$$y^{(n)}(x) = f\left(x, y(x), y'(x), \ldots, y^{(n-1)}(x)\right), \tag{1}$$

where $y'(x)$, …, $y^{(m-1)}(x)$, $y^{(m)}(x)$ – the successive derivatives of a function $y(x)$, with boundary conditions assumed for $x = 0$ and $x = x_{O_2}$ (i.e. at the origin and the end points of the designed geometrical layout).

A number and type of the boundary conditions are dependent on the requirements imposed on the curve. A number of the boundary conditions determines the order of a differential equation.

Fig. 1 in the point O, the following boundary conditions are assumed:

$$y(0) = y'(0) = 0;\ \ y''(0) = k_1;\ \ y'''(0) = k_1', \tag{2}$$

where k_1 – value of curvature at a point O; k_1' – value of the first derivative of curvature at point O.

The appropriate boundary conditions are assumed at the point O_2 (where in k_2 and k_2' stand for the value of a curvature and a value of the first derivative of a curvature while θ_{O_2} stands for the slope of the tangent at that point):

$$\begin{cases} y(x_{O_2}) = y_{O_2} \\ y'(x_{O_2}) = \tan\theta_{O_2} \\ y''(x_{O_2}) = k_2\left(\sqrt{1+\tan^2\theta_{O_2}}\right)^3 \\ y'''(x_{O_2}) = k_2'\left(\sqrt{1+\tan^2\theta_{O_2}}\right)^3 + 3k_2^2\tan\theta_{O_2}\left(1+\tan^2\theta_{O_2}\right)^2 \end{cases}. \tag{3}$$

Several examples of an application of the presented method have been described in the paper of Koc and Mieloszyk (1998). Whereas, as proved in the mentioned paper, the serious limits have appeared: the curvature monotonicity condition has not always been fulfilled. It turned out that the obtained results are useful only in the restricted range of values of the parameters. Very high sensitivity of the solutions to slight the changes of values of geometrical layout parameters has been observed (Koc, Palikowska 2012). The method is not the universal one; the appropriate functions are adjusted separately to individual cases.

Therefore, the appropriate approach to a problem is to focus on curvature modelling. As a result of the curvature modelling, the unambiguous and advantageous solution identifying the transition curve is possible to obtain. However, it should be taken into account that the curvature modelling forces the necessity of adjusting the position of a curve K_2 (a position of the curve K_2 cannot be set as an entry parameter in the process of a geometrical layout design regrettably).

3. General method of modelling curvature

Similarly as previously, as a result of generalization of the lateral unbalanced acceleration identification regarding to different types of the transition curves (Mieloszyk, Koc 1991), the curvature function $k(l)$ is being searched among the solutions of the following differential equation:

$$k^{(m)}(l) = f\left[l, k(l), k'(l), \ldots, k^{(m-1)}(l)\right], \tag{4}$$

where l – arc length from the original point of a curve to the chosen point along the curve; $k'(l)$, ..., $k^{(m-1)}(l)$, $k^{(m)}(l)$ – successive derivatives of the curvature function $k(l)$, with boundary conditions at the original point (for $l = 0$) and at the final point (for $l = l_k$) of the transition curve.

The boundary conditions are:

$$k^{(i)}(0^+) = \begin{cases} k_2 & \text{for } i = 0 \\ 0 & \text{for } i = 1,\ 2,\ \ldots,\ n_1 \end{cases}, \tag{5}$$

$$k^{(j)}(l_k^-) = \begin{cases} k_2 & \text{for } j = 0 \\ 0 & \text{for } j = 1,\ 2,\ \ldots,\ n_2 \end{cases}. \tag{6}$$

The differential Eq (4) order is $m = n_1 + n_2 + 2$ while the obtained curvature function $k(l)$ is of a class C^n in the range $\langle 0, l_k\rangle$, where $n = \min(n_1, n_2)$. The presented method enables joining route segments of a different curvature. An introduction of the signed curvature enables the joint of two circular arcs with the radii R_1 (m) and R_2 (m), both with C-shaped transition curve (e.g., $k_1 = \frac{rad}{R_1}$, $k_2 = \frac{rad}{R_2}$) and S-shaped transition curve (e.g., $k_1 = \frac{rad}{R_1}$, $k_2 = -\frac{rad}{R_2}$).

3.1. Linear curvature changes (K^0 curve)

As it is known, the linear curvature change occurs on a transition curve named clothoid, often used in the highway alignment, joining a straight route segment ($k_1 = 0$) with a circular arc segment ($k_2 = \frac{rad}{R_2}$).

It is premised that the linear curvature change on the specified transition curve length l_k is obtained as a result of the assumption of two elementary boundary conditions (in the generalized approach of the presented case):

$$\begin{cases} k(0^+) = k_1 \\ k(l_k^-) = k_2 \end{cases} \tag{7}$$

and the differential Eq (8) is as follows:

$$k''(l) = 0. \tag{8}$$

After determining the constants, the solution of the differential Eqs (7)–(8) is as follows:

$$k(l) = k_1 + \frac{1}{l_k}(k_2 - k_1)l. \tag{9}$$

Since the resulting solution (9) is a function of the class C^0, it is included in the category referred as the K^0 curves.

The primary task is to determine the coordinates of the curve described by the curvature (9) in a Cartesian coordinate system x, y. It is assumed that the original point O of the system is located at the end point of the curve with the curvature k_1 and x axis is tangent to the curve at that point (Fig. 1). The formula of the desired transition is written in parametric form:

$$x(l) = \int \cos\theta(l)\, dl, \tag{10}$$

$$y(l) = \int \sin\theta(l)\, dl. \tag{11}$$

The parameter l represents a current position of the chosen point along the curve length. The function of slope of the tangent $\theta(l)$ is defined by the formula:

$$\theta(l) = \int k(l)\, dl. \tag{12}$$

In the presented case:

$$\theta(l) = k_1 l + \frac{1}{2l_k}(k_2 - k_1)l^2. \tag{13}$$

The determination of $x(l)$ and $y(l)$ using formulas (10) and (11) requires, in a general case, an expansion of the integrands in the Taylor series, and the mentioned case in the Maclaurin series.

As a result of the expansion procedure, the following parametric equations are obtained as follow:

$$x(l) = \int \cos\theta(l)dl = l - \frac{k_1^2}{6}l^3 - \frac{k_1}{8l_k}(k_2 - k_1)l^4 + \left[\frac{k_1^4}{120} - \frac{1}{40l_k^2}(k_2 - k_1)\right]l^5 + \frac{k_1^3}{72l_k}(k_2 - k_1)l^6 - \left[\frac{k_1^6}{5040} - \frac{k_1^2}{112l_k^2}(k_2 - k_1)^2\right]l^7 - \left[\frac{k_1^5}{1920l_k}(k_2 - k_1) - \frac{k_1}{384l_k^3}(k_2 - k_1)^3\right]l^8 + \left[\frac{k_1^8}{362880} - \frac{k_1^4}{1728l_k^2}(k_2 - k_1)^2 + \frac{1}{3456l_k^4}(k_2 - k_1)^4\right]l^9 \ldots. \tag{14}$$

$$y(l) = \int \sin\theta(l)dl = \frac{k_1^2}{2}l^2 + \frac{1}{6l_k}(k_2 - k_1)l^3 - \frac{k_1^3}{24}l^4 - \frac{k_1^2}{20l_k}(k_2 - k_1)l^5 + \left[\frac{k_1^5}{720} - \frac{k_1}{48l_k^2}(k_2 - k_1)^2\right]l^6 + \left[\frac{k_1^4}{336l_k}(k_2 - k_1) - \frac{1}{336l_k^3}(k_2 - k_1)^3\right]l^7 - \left[\frac{k_1^7}{40320} - \frac{k_1^3}{384l_k^2}(k_2 - k_1)^2\right]l^8 - \left[\frac{k_1^6}{12960l_k}(k_2 - k_1) - \frac{k_1^2}{864l_k^3}(k_2 - k_1)^3\right]l^9 \ldots. \tag{15}$$

It is easy to ensure that the above parametric equations for $k_1 = 0$ describe a clothoid transitional curve. In the *S*-shaped transition case (i.e. reverse curvatures, curvatures with different signs), however, a problem with the monotonic course of the function $\theta(l)$ appears. In the *C*-shaped transition case (i.e. *sign* k_1 = *sign* k_2) function $\theta(l)$ is a monotonic one, while in the *S*-shaped transition case on the graph of the function $\theta(l)$ an extremum appears at the point l_0 (Fig. 2), in which:

$$\theta'(l_0) = k(l_0) = k_1 + (k_2 - k_1)\frac{l_0}{l_k} = 0. \tag{16}$$

The values of l_0 and $\theta(l_0)$ result from the following relationships:

$$l_0 = -\frac{k_1}{k_2 - k_1}l_k, \tag{17}$$

$$\theta(l_0) = -\frac{k_1^2}{2(k_2 - k_1)}l_k. \tag{18}$$

In the presented case the parametric Eqs (14) and (15) for the transition curve are valid for $l \in \langle 0, l_0\rangle$; for $l \in (l_0, l_k\rangle$ after expansion of the functions cos $\theta(l)$ and

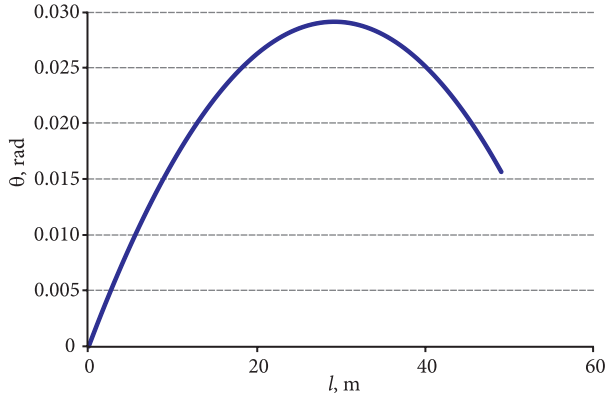

Fig. 2. Slope of the tangent $\theta(l)$ chart, described by formula (13), for *S*-shaped joining of circular arcs with curvatures $k_1 = \frac{1}{500}$ rad/m and $k_2 = -\frac{1}{700}$ rad/m (l_k = 50 m)

$\sin\theta(l)$ in Taylor series and integration the following parametric equations are obtained:

$$x(l)=\int\cos\theta(l)dl=x(l_0)+\cos\left(-\frac{k_1^2}{2(k_2-k_1)}l_k\right)(l-l_0)-\left[\frac{k_2-k_1}{6l_k}\sin\left(-\frac{k_1^2}{2(k_2-k_1)}l_k\right)\right](l-l_0)^3-\left[\frac{(k_2-k_1)^2}{40\,l_k^2}\cos\left(-\frac{k_1^2}{2(k_2-k_1)}l_k\right)\right](l-l_0)^5+\left[\frac{(k_2-k_1)^3}{336\,l_k^3}\sin\left(-\frac{k_1^2}{2(k_2-k_1)}l_k\right)\right](l-l_0)^7+\ldots. \quad (19)$$

$$y(l)=\int\sin\theta(l)dl=y(l_0)+\sin\left(-\frac{k_1^2}{2(k_2-k_1)}l_k\right)(l-l_0)+\left[\frac{k_2-k_1}{6l_k}\cos\left(-\frac{k_1^2}{2(k_2-k_1)}l_k\right)\right](l-l_0)^3-\left[\frac{(k_2-k_1)^2}{40\,l_k^2}\sin\left(-\frac{k_1^2}{2(k_2-k_1)}l_k\right)\right](l-l_0)^5-\left[\frac{(k_2-k_1)^3}{336\,l_k^3}\cos\left(-\frac{k_1^2}{2(k_2-k_1)}l_k\right)\right](l-l_0)^7+\left[\frac{(k_2-k_1)^4}{3456\,l_k^4}\sin\left(-\frac{k_1^2}{2(k_2-k_1)}l_k\right)\right](l-l_0)^9+\ldots. \quad (20)$$

The correct solution in the *S*-shaped transition case (Fig. 3) is obtained using two pairs of the parametric equations:

– the pair of the formulas (14) and (15) for $l\in\langle 0, l_0\rangle$;

– the pair of the formulas (19) and (20) for $l\in(l_0, l_k\rangle$.

From a practical point of view, it is very important to determine the value of the slope of the tangent at the end of the transitional curve. It equals:

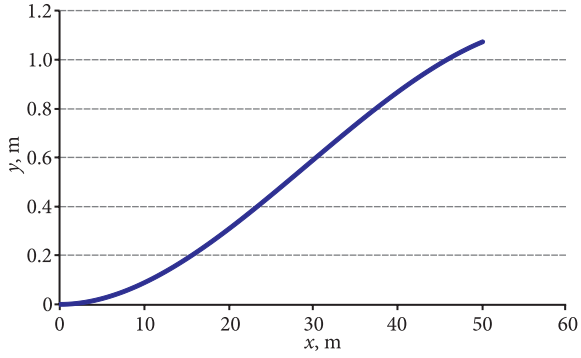

Fig. 3. Horizontal ordinates $y(x)$ chart, described by the formulas (14), (15), (19) and (20) for *S*-shaped joining of circular arcs with curvatures $k_1=\frac{1}{500}$ rad/m and $k_2=-\frac{1}{700}$ rad/m ($l_k=50$ m)

$$\theta(l_k)=\frac{1}{2}(k_1+k_2)l_k. \quad (21)$$

Determination of the value $\theta(l_k)$ enables joining of the transitional curve *K* with the curve K_2, fulfilling the condition of both curves tangent conformity at the joining point.

3.2. Nonlinear curvature changes (K^1 curve)

As presented in section 3.1, the solution for a linear curvature change is unambiguous and unique, nonlinear solutions, obtained assuming different boundary conditions and different forms of differential equation, are various.

The nonlinear case, which refers to the classical transition curves joining the straight route segment with the circular arc segment, identified as Bloss curve (Mieloszyk, Koc 1991), has been considered.

The following boundary conditions have been adopted:

$$\begin{cases}k(0^+)=k_1, & k(l_k^-)=k_2\\ k'(0^+)=0, & k'(l_k^-)=0\end{cases} \quad (22)$$

the differential equation is as follows:

$$k^{(4)}l=0. \quad (23)$$

As a result of solving the differential Eqs (22), (23) the following formula $k(l)$, describing the curvature of the transition curve, has been obtained:

$$k(l)=k_1+\frac{3}{l_k^2}(k_2-k_1)l^2-\frac{2}{l_k^3}(k_2-k_1)l^3. \quad (24)$$

Since the obtained solution (24) is a function of C^1 class, it is included in the category referred as the K^1 curves.

The slope of the tangent function $\theta(l)$ is defined by the formula:

$$\theta(l)=k_1l+\frac{1}{l_k^2}(k_2-k_1)l^3-\frac{1}{2l_k^3}(k_2-k_1)l^4. \quad (25)$$

The following parametric equations have been obtained after the function $\cos\theta(l)$ and $\sin\theta(l)$ expansion in Maclaurin series and integration of them:

$$x(l)=\int\cos\theta(l)dl=l-\frac{k_1^2}{6}l^3+\left[\frac{k_1^4}{120}-\frac{k_1}{5l_k^2}(k_2-k_1)\right]l^5+\frac{k_1}{123l_k^3}(k_2-k_1)l^6-\left[\frac{k_1^6}{5040}-\frac{k_1^3}{42l_k^2}(k_2-k_1)+\frac{1}{14l_k^4}(k_2-k_1)^2\right]l^7-\left[\frac{k_1^3}{96l_k^3}(k_2-k_1)-\frac{1}{16l_k^5}(k_2-k_1)^2\right]l^8+\left[\frac{k_1^8}{362880}-\frac{k_1^5}{1080l_k^2}(k_2-k_1)+\frac{k_1^2}{36l_k^4}(k_2-k_1)^2+\frac{1}{72l_k^6}(k_2-k_1)^2\right]l^9+\ldots, \quad (26)$$

$$y(l)=\int \sin\theta(l)\,dl=\frac{k_1}{2}l^2-\left[\frac{k_1^3}{24}-\frac{1}{4l_k^2}(k_2-k_1)\right]l^4-\frac{1}{10l_k^3}(k_2-k_1)l^5+\left[\frac{k_1^5}{720}-\frac{k_1^2}{12l_k^2}(k_2-k_1)\right]l^6+\frac{k_1^2}{28l_k^3}(k_2-k_1)l^7-\left[\frac{k_1^7}{40320}-\frac{k_1^4}{192l_k^2}(k_2-k_1)+\frac{k_1}{16l_k^4}(k_2-k_1)^2\right]l^8+\left[\frac{k_1}{18l_k^5}(k_2-k_1)^2-\frac{k_1^4}{432l_k^3}(k_2-k_1)\right]l^9+\ldots. \quad (27)$$

Assuming that $k_1 = 0$, the parametric Eqs (26) and (27) identify the Bloss curve.

The nonlinear curvature $k(l)$, in the case of *C*-oval transition, has been presented (one of the circular arcs lies partly inside the other) in Fig. 4.

In *S*-shaped transition case (i.e. *sign* $k_1 \neq$ *sign* k_2) on the chart of the function $\theta(l)$ an extremum appears in the point l_0, in which:

$$\theta'(l_0)=k_1+\frac{3}{l_k^2}(k_2-k_1)l_0^2-\frac{2}{l_k^3}(k_2-k_1)l_0^3=0. \quad (28)$$

The parametric Eqs (26) and (27) of the transition curve are valid for $l \in \langle 0, l_0\rangle$. As a result of solving the 3rd degree of Eq (28), the following formula for the value l_0 has been obtained:

$$l_0=\left[\frac{1}{2}-\cos\left(\frac{\varphi}{3}+\frac{\pi}{3}\right)\right]l_k, \quad (29)$$

where the angle φ values result from the relationship:

$$\cos\varphi=\frac{k_1+k_2}{k_2-k_1}. \quad (30)$$

The transitional curve's parametric equations for $l \in (l_0, l_k\rangle$ are determined by expanding the functions $\cos\theta(l)$ and $\sin\theta(l)$ in Taylor series. By the usage of formulas (26) and (27), the correct solution for the *S*-shaped transitional case has been obtained (Fig. 5).

The slope of the tangent θ at the end of the transition curve, enabling to join the transition curve *K* with the curve K_2 with fulfilment of the condition of both curves tangent conformity at the joining point, is analogous to the linear curvature case (Section 3.1.) i.e. it is described by the formula (21).

3.3. Methodology of K^0 and K^1 curves evaluation

In order to evaluate the properties of K^0 and K^1 curves, these solutions will be compared to another known curves, which curvature functions $k(l)$ belong to the similar continuity class (i.e. they have the similar degree of the smoothness) and at joining points with the arcs the obtained transitions have at least G^2 continuity. As the reference curves, two families of Bezier curves, presented in Section 4, have been chosen.

Two evaluation methods of the dynamic properties of K^0 and K^1 curves versus to the mentioned Bezier curves have been applied. The first method, presented by Koc and Mieloszyk (1998), is based on the dynamic model and the estimation of the dynamic effects. An essential goal of the dynamic analysis is to determine the function of oscillations $X(t)$ and resultant acceleration of oscillating motion $X''(t)$ in areas where changes of horizontal curvature of the route occur.

The second method of the evaluation of dynamic effects is based on the Lateral Change of Acceleration criterion (LCA diagram) presented in the papers Baykal (1996) and Tari (2003). The evaluation of LCA enables the determination of the conformity of horizontal geometry of route related to the vehicle-road dynamics.

The evaluation results, obtained using both methods, are presented in Section 5.

4. Bezier curves

Two curves of Bezier family, cubic *C*-Bezier curves (Cai, Wang 2009) and Pythagorean hodograph quintic Bezier curves (Habib, Sakai 2007a) have been chosen. Both families allow to ensure the monotonicity condition of the curvature function (*S*-shaped transition).

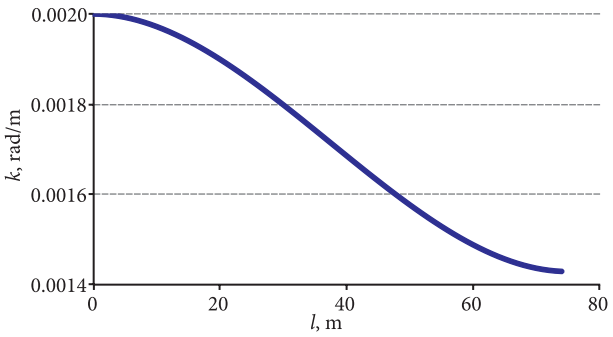

Fig. 4. Nonlinear curvature $k(l)$ chart for *C*-oval joining of circular arcs with curvatures $k_1 = \frac{1}{500}$ rad/m and $k_2 = \frac{1}{700}$ rad/m ($l_k = 75$ m)

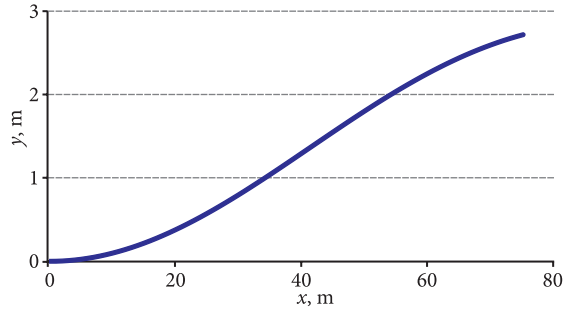

Fig. 5. Horizontal ordinates $y(x)$ chart for *S*-shaped joining the circular arcs with curvatures $k_1 = \frac{1}{500}$ rad/m and $k_2 = -\frac{1}{700}$ rad/m ($l_k = 75$ m)

4.1. Cubic *C*-Bezier curve

The family of cubic *C*-Bezier curves has been proposed for G^2 continuity of joining two circular arcs by a single-segment curve in a highway route design, in the paper (Cai, Wang 2009). Cubic *C*-Bezier curves are used for joining two circular arcs with *S*-shaped (i.e. arcs with reverse curvature), *C*-oval (i.e. arcs with conform curvature when one of the arcs lies partly inside the other) and broken back *C*-shaped transitions (i.e. non-enclosing arcs with conform curvatures).

Cubic *C*-Bezier curve has been defined as:

$$P(t)=\frac{2}{\pi-2}\begin{bmatrix}\sin t\\ \cos t\\ t\\ 1\end{bmatrix}^{T}\begin{bmatrix}0 & \frac{2-\pi}{4-\pi} & \frac{2}{4-\pi} & -1\\ -1 & \frac{2}{4-\pi} & \frac{2-\pi}{4-\pi} & 0\\ -1 & \frac{2}{4-\pi} & \frac{-2}{4-\pi} & 1\\ \frac{\pi}{2} & \frac{-2}{4-\pi} & \frac{\pi-2}{4-\pi} & 0\end{bmatrix}\begin{pmatrix}P_0\\ P_1\\ P_2\\ P_3\end{pmatrix} \tag{31}$$

for the parameter t in the interval $0\le t\le\frac{\pi}{2}$. Among control points $\{P_i\}_{i=0}^{3}$ of Bezier curve, points P_0 and P_3 are at the same time Bezier nodes and the tangency points of the curve and the arcs (Figs 6 and 7).

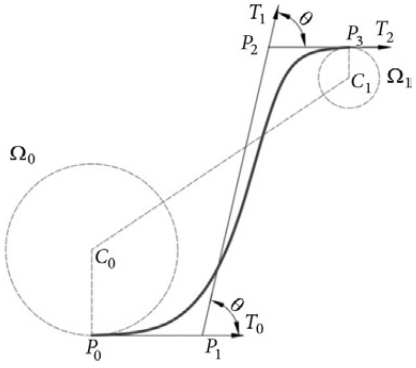

Fig. 6. Schema of *S*-shaped joining of the circular arcs using a cubic *C*-Bezier curve

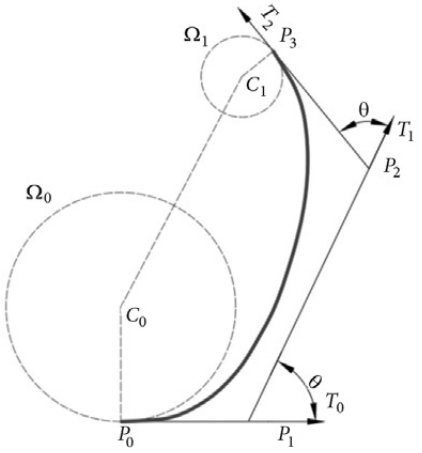

Fig. 7. Schema of *C*-shaped joining of the circular arcs using a cubic *C*-Bezier curve

The algorithm for determination of the control points $\{P_i\}_{i=0}^{3}$ has been presented in the paper Cai and Wang (2009). The algorithm takes into account the geometrical parameters of the designed layout (i.e. arc radii and the position of the arc centres C_0 and C_1). The unit vectors T_i corresponding with control points P_i determine the value of the angle θ (Figs 6 and 7).

The first and second derivatives of $P(t)$ are:

$$P'(t)=mR_0\tan\theta\Big[\big(1-\sin t\big)T_0+m\big(\cos t+\sin t-1\big)\sec\theta T_1+\lambda\big(1-\cos t\big)T_2\Big], \tag{32}$$

$$P''(t)=mR_0\tan\theta\Big[-\cos tT_0+m\big(\cos t-\sin t\big)\sec\theta T_1+\lambda\sin tT_2\Big], \tag{33}$$

where a shape parameter m – introduced and the relationship between arc radii is represented by a parameter $\lambda=\sqrt{\frac{R_0}{R_1}}$.

In the case of *S*-shaped transition (i.e. a case of the reverse curvatures of two circular arcs) one of two pairs of relationship is between m and l:

1) $m\ge\frac{2}{3}$ and $\frac{1}{3}\le\lambda\le 1$ or

2) $m\ge 1$ and $\frac{1}{7}\le\lambda\le 1$.

It has to be satisfied in order to ensure the monotonic curvature of the obtained solution.

In the case of *C*-shaped transition (i.e. a case of the conform curvatures of two non-enclosing circular arcs), when a relationship $m\ge\frac{(1+\sqrt{7})}{3}$ is fulfilled, the obtained curvature has a single extremum (the monotonicity condition cannot be satisfied). The monotonicity condition is satisfied in the case of *C*-oval transition, in which one of the circular arcs lies inside the other.

It should be outlined that the algorithm ensures that a single-segment transition is obtained without changes of the position of the arc centres C_0 and C_1.

4.2. Quintic Bezier curve

Pythagorean hodograph (abbreviated further as PH) Bezier curves have been presented in the papers Habib and Sakai (2007a) and (2007b). Quintic Bezier curve is given as:

$$P(t)\big(=x(t),y(t)\big)=\sum_{i=0}^{5}\binom{5}{i}P_i\big(1-t\big)^{5-i}t^i \tag{34}$$

to a parameter t in the interval $0\le t\le 1$. Among the control points $\{P_i\}_{i=0}^{5}$ of Bezier curve, points P_0 and P_5 are at the same time Bezier nodes and the tangency points of the curve and the arcs (Figs 8 and 9).

The presented curve is assumed to be a Pythagorean hodograph curve as its $x'(t)^2+y'(t)^2$ is expressed as the square of a polynomial in t. To ensure this, the first derivative is defined as:

$$P'(t)\big(=x'(t),y'(t)\big)=\Big(u^2(t)-v^2(t),2u(t)v(t)\Big), \quad (35)$$

where

$$u(t)=u_0\big(1-t\big)^2+2u_1t\big(1-t\big)+u_2t^2, \quad (36)$$

$$v(t)=v_0\big(1-t\big)^2+2v_1t\big(1-t\big)+v_2t^2. \quad (37)$$

The algorithm of the construction of PH quintic Bezier curve consists of determination of the control points $\{P_i\}_{i=0}^5$ on the basis of coefficients u_0, u_1, u_2 and v_0, v_1, v_2, taking into account the shape parameter m and the distance R between the centres of the arcs Ω_0 and Ω_1 (Figs 8 and 9).

In all cases *S*-shaped, *C*-oval and *C*-shaped transitions specifying relationships between geometrical parameters are met to ensure that the obtained solution has the monotonic curvature (*S*-shaped and *C*-oval) or a single extremum curvature (*C*-shaped).

Unfortunately, as a result of the construction of PH quintic Bezier curve, the position of the centre C_1 of the arc Ω_1 varies. Only the distance $\|C_1-C_0\|$ between the centres of the arcs is constant. This restriction is the disadvantage in a comparison with the construction of a cubic *C*-Bezier curve. It has ensured a constant position of both centres C_0 and C_1 of the arcs Ω_0 and Ω_1.

5. Analysis of the dynamic properties

In order to compare the dynamic properties of the mentioned curves, the case of geometrical layout of two circular arcs Ω_0 and Ω_1 with reverse curvature has been considered (Table 1).

As a result of inscribing K^0 curve of the assumed length l_k = 600 m in the geometrical layout presented in Table 1, the position of the centre C_1 = (583.109; –572.33) of the arc Ω_1 and the distance $\|C_1-C_0\|$ = 1220.61 m between the centres of the arcs have been obtained.

Next, preserving the position of the centres C_0 and C_1 for different values of shape parameter $m \in \{0.7; 1; 2\}$, the family of cubic *C*-Bezier curves has been constructed.

Then, taking the position of the centre C_0 of the arc Ω_0 and obtained distance $\|C_1-C_0\|$ = 1220.61 m, the shape parameter m = 0.895, which guarantees the monotonic curvature of the obtained transition, has been adjusted.

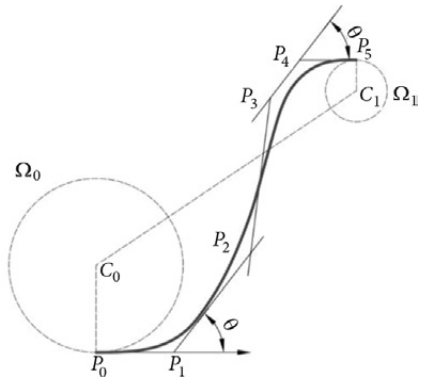

Fig. 8. Schema of *S*-shaped joining of the circular arcs using PH quintic Bezier curve

The similar coordinates of the points of tangency between curves and the arc Ω_1 and similar positions of the centre C_1 of the arc have been obtained. Finally, as a result of construction of K^1 curve of the length l_k = 600 m, the position of the centre C_1 = (615.11; –550.91) has been obtained.

The constructed curves are presented in Fig. 10.

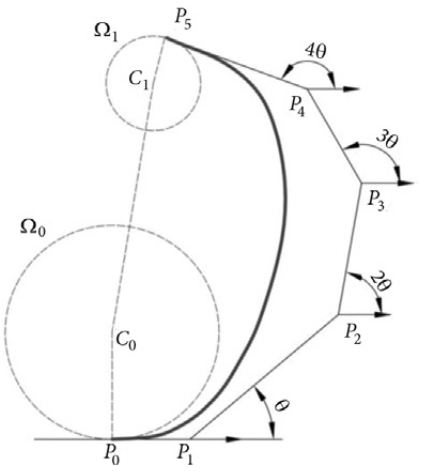

Fig. 9. Schema of *C*-shaped joining of the circular arcs using PH quintic Bezier curve

Table 1. Parameters of the geometrical layout of two circular arcs Ω_0 and Ω_1 with a reverse curvature (i.e. *sign* $k_1 \neq$ *sign* k_2)

Position of the centre of the arc		Arc radius	
C_0	(0; 500)	R_0	500 m
C_1	determined as result of the construction algorithm	R_1	700 m

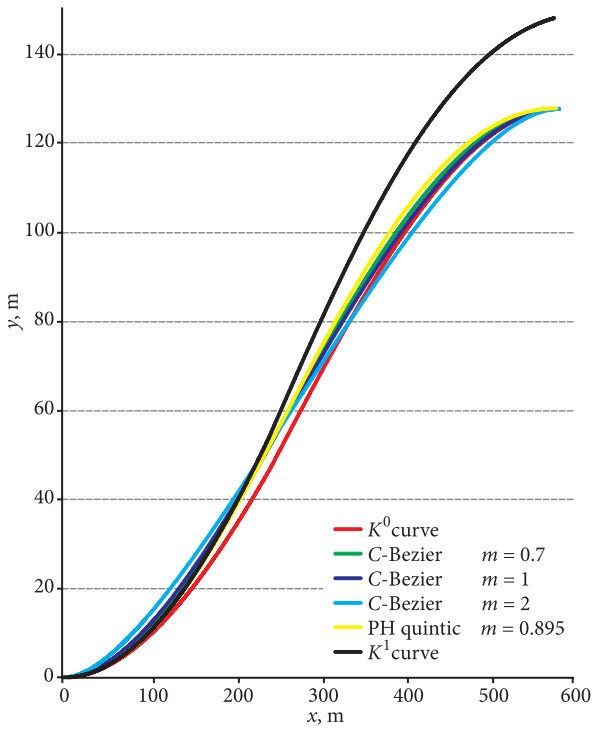

Fig. 10. Horizontal ordinates *y(x)* chart for *S*-shaped curves

The geometrical parameters of the constructed *S*-shaped curves are presented in Table 2.

In order to evaluate the dynamic properties of the presented curves (Table 2), the functions of oscillations $X(t)$ and resultant acceleration of oscillating motion $X''(t)$ have been determined. It has been assumed that the function of lateral unbalanced acceleration $a(l)$ along the transition curve, as proved by Koc and Mieloszyk (1998), results directly from the function of a curvature $k(l)$:

$$a(l) = a_{\max} k(l) \frac{R}{rad}, \tag{38}$$

where R – radius of the circular arc; $a_{\max}$ – value of lateral unbalanced acceleration on the circular arc.

Lateral unbalanced acceleration along the transition curves, described in Table 2, is presented in Fig. 11.

Basing on the assumption that horizontal curvature changes are a forcing factor of the lateral oscillations, a numerical method for determination of the function of oscillations $X(t)$ has been presented in the paper (Koc, Palikowska 2012).

The following values of the parameters have been assumed (for rail vehicle):

– free vibration frequency ω = 3.51 1/s;
– Lehr damping coefficient D = 0.175;
– constant velocity v = 120 km/h;
– lateral unbalanced accelerations $a_{0\max}$ = 0.6 m/s^2 and
– $a_{1\max}$= –0.43 m/s^2 on the arcs Ω_0 and Ω_1.

The resultant acceleration of oscillation motion $X''(t)$ for compared curves has been presented in Fig. 12. Taking into account the maximum values of resultant acceleration of oscillation motion $X''(t)$, K^1 curve has the most convenient dynamic properties. Cubic *C*-Bezier curve with the shape parameter m = 0.7 and PH quintic Bezier curve have similar dynamic properties, which are assessed as more favourable than the properties of K^0 curve.

Apart from the evaluation based on resultant acceleration of oscillating motion $X''(t)$, the analysis of LCA has been carried out. LCA is the change of resultant acceleration occurring along the curve normal respect to time. The resultant acceleration is formed by the free forces acted on a vehicle (with a mass m and an instantaneous velocity v) moving on a curved orbit (Baykal 1996; Tari 2003).

Three functions: $v=v(l)$ – function of velocity related to the road, $k=k(l)$ – function of curvature related to the road and $u=u(l)$ – function of super elevation related to

Table 2. Parameters of the constructed *S*-shaped curves

Curve	K^0	K^1	PH quantic	*C*-Bezier	
Shape parameter, m	–	–	0.895	0.7	1
Curve length l, m	600	600	597.05	599.98	599.54
Tangency point $(x; y)$	(583.05; 127.67)	(577.45; 148.08)	(579.59; 127.82)	(583.09; 127.67)	(583.09; 127.67)
C_1 $(x; y)$	(583.33; –572.33)	(615.11; –550.91)	(583.09; –572.18)	(583.09; –572.33)	(583.09; –572.33)

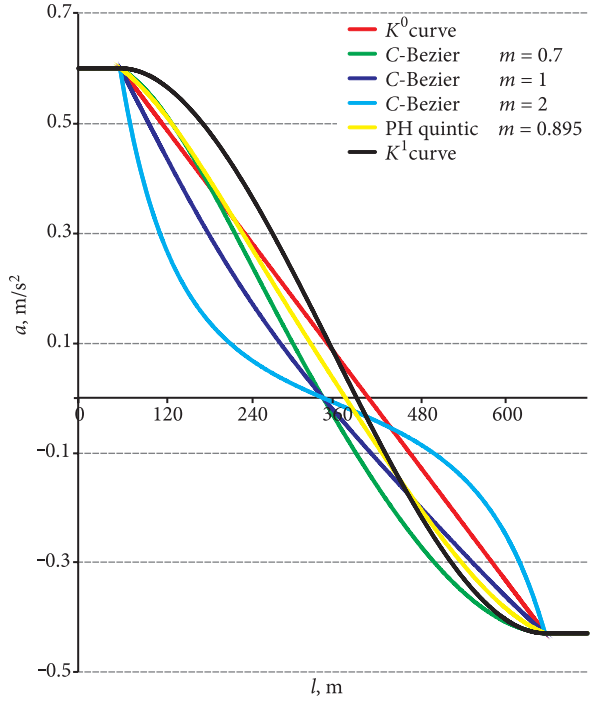

Fig. 11. Lateral unbalanced acceleration along the *S*-shaped curves

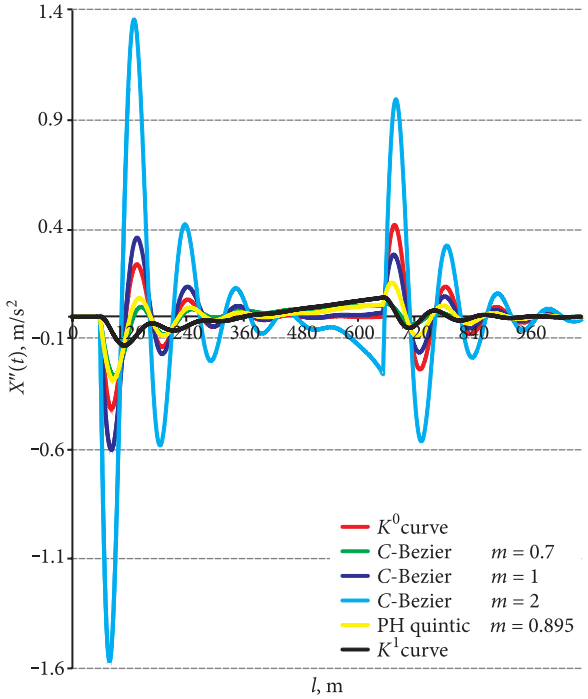

Fig. 12. Acceleration of oscillating motion X'' as a function of curve length l

the road, are needed to derive the function of LCA for any curve using the formula (39):

$$LCA = \frac{pv}{\sqrt{u^2 + p^2}} \left(3ka_t + v^2 \frac{dk}{dl} - \frac{kv^2 u + gp}{u^2 + p^2} \cdot \frac{du}{dl} \right), \quad (39)$$

where p – horizontal width of the road platform; a_t – tangential acceleration produced by motor force; l – arc length measured from the origin point of the curve to the chosen point on the route; g – gravity constant.

LCA diagram for compared curves is presented in Fig. 13. The motion model with constant velocity v = 120 km/h, maximum value of super elevation $u_{0\max}$ = 0.15 m and $u_{1\max}$ = 0.11 m on the arcs Ω_0 and Ω_1 respectively and gravity constant g = 9.81 m/s^2 have been assumed.

Three main criteria of evaluation of the dynamic properties of the transition curves based on LCA diagram have been suggested in the paper Tari (2003), based on the first of Tari criteria and examination of the continuity of LCA function, It is concluded that only K^1 curve satisfies the condition of continuity.

This proves that K^1 curve is superior to other curves which have discontinuities at the joining points (i.e. tangency points curve-arc). Discontinuities in the form of jump on the cubic *C*-Bezier curve with a shape parameter m = 0.7 and PH quintic Bezier curve are characterized by the smallest values in comparison to other curves. According to Tari (2003), the presented advantage of K^1 curve is sufficient to prefer K^1 curve to other curves.

The second criterion compares the extreme values of LCA, taking into account that values of LCA are greater or equal than 0.3 m/s^3 which are felt by humans, while a value of LCA = 0.6 m/s^3 is the threshold value above which humans feel uncomfortably.

Maximum value of LCA for K^1 curve is slightly above the passenger feeling threshold, while for cubic *C*-Bezier curve with a shape parameter m = 0.7 and PH quintic Bezier curve is below this threshold. Although, the second criterion prefers Bezier curves to K^1 curve, the dominant role in comparison has a conclusion from the first one.

The third criterion examines differences between the slope values of the two tangents on the diagram of LCA at the points where different route elements join. It is only useful in the cases when the compared curves are found equivalent regarding the first and the second criteria.

6. Conclusions

1. A general method of modelling the curvature of a highway route using differential equations is presented in the paper. The method enables to join route segments of different curvature. The advantage of the method consists of identifying analytical solution which belongs to the assumed class depending on the order of differential equation.

2. The presented method enables to identify the different types of transitional curves. A solution for linear curvature change (K^0 curve) and selected nonlinear case (K^1 curve) have been presented in the case of *S*-shaped and *C*-oval transitions. The single-segment transitions which satisfy a monotonicity condition of the curvature have been obtained in all cases.

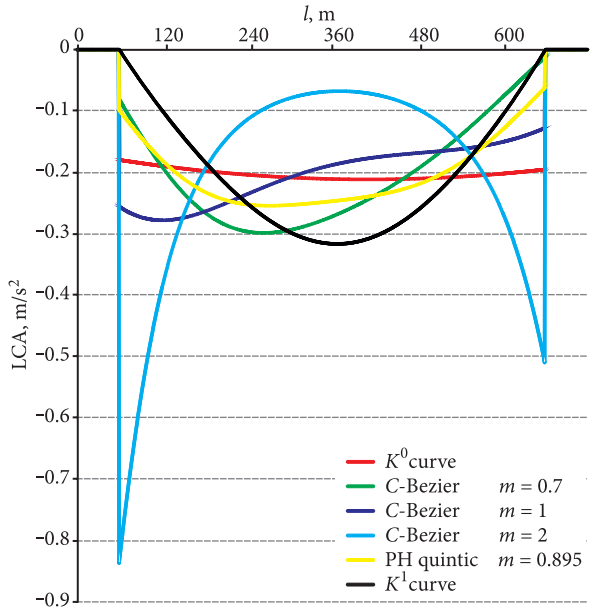

Fig. 13. LCA diagram of the *S*-shaped curves in motion model with constant velocity

3. The obtained transitional curves have been compared with a family of cubic *C*-Bezier curves and PH quintic Bezier curve using the mentioned curves as transition curves, joining two circular arcs with the reverse curvature (i.e. *S*-shaped transition). The similar length of the curves $l_k \approx$ 600 m and similar positions of the tangency point curve-arc and the centre C_1 of the arc Ω_1 have been obtained in the geometrical layout used for comparison. The algorithm of construction of cubic *C*-Bezier curve has appeared to be the most flexible one. It preserves the position of the centres C_0 and C_1 of the arcs Ω_0 and Ω_1, and it has the least restrictive geometrical conditions for existing of the solution.

4. The analysis of dynamic properties has been based on two methods and led to the conclusion that K^1 curve has the most advantageous vehicle-road dynamic properties among the compared curves. Slightly, less favourable properties have been identified with regard to cubic *C*-Bezier curve with the properly adjusted shape parameter (m = 0.7) and PH quintic Bezier curve. Both of the above mentioned curves have better dynamic properties than K^0 curve.

5. The analysis has proved that transitions, characterized by linear curvature changes (i.e. spiral curves), are inferior to nonlinear solutions and they are not adequate for the road dynamics. The application of linear curvatures in a highway alignment has no further justification.

References

Ahmad, A.; Ali, J. 2008. G^3 Transition Curve between Two Straight Lines, in *Proc. of the 5th International Conference on Computer Graphics, Imaging and Visualisation,* 26–28 August 2008, 154–159. http://dx.doi.org/10.1109/CGIV.2008.22

Baykal, O. 1996. On Concept of Lateral Change of Acceleration, *Journal of Surveying Engineering* 122(3): 132–141. http://dx.doi.org/10.1061/(ASCE)0733-9453(1996)122:3(132)

Bosurgi, G.; Pellegrino, O.; Sollazzo, G. 2016. Using Genetic Algorithms for Optimizing the PPC in the Highway Horizontal Alignment Design, *Journal of Computing in Civil Engineering* 30(1). http://dx.doi.org/10.1061/(ASCE)CP.1943-5487.0000452

Bosurgi, G.; D'Andrea, A. 2012. A Polynomial Parametric Curve (PPC-Curve) for the Design of Horizontal Geometry of Highways, *Computer-Aided Civil and Infrastructure Engineering* 27(4): 304–312. http://dx.doi.org/10.1111/j.1467-8667.2011.00750.x

Cai, H.; Wang, G. 2009. A New Method in Highway Route Design: Joining Circular Arcs by a Single C-Bezier Curve with Shape Parameter, *Journal of Zhejiang University SCIENCE A* 10(4): 562–569. http://dx.doi.org/10.1631/jzus.A0820267

Habib, Z.; Sakai, M. 2007a. G^2 Pythagorean Hodograph Quintic Transition between Two Circles with Shape Control, *Computer-Aided Geometric Design* 24(5): 252–266. http://dx.doi.org/10.1016/j.cagd.2007.03.004

Habib, Z.; Sakai, M. 2007b. On PH Quantic Spirals Joining Two Circles with One Circle Inside the Other, *Computer-Aided Design* 39(2): 125–132. http://dx.doi.org/10.1016/j.cad.2006.10.006

Kobryń, A. 2014. New Solutions for General Transition Curves, *Journal of Surveying Engineering* 140(1): 12–21. http://dx.doi.org/10.1061/(ASCE)SU.1943-5428.0000113

Kobryń, A. 2011. Polynomial Solutions of Transition Curves, *Journal of Surveying Engineering* 137(3): 71–80. http://dx.doi.org/10.1061/(ASCE)SU.1943-5428.0000044

Koc, W. 2014. Analytical Method of Modelling the Geometric System of Communication Route, *Mathematical Problems in Engineering*, ID 679817, 13 p. http://dx.doi.org/10.1155/2014/679817

Koc, W.; Chrostowski, P. 2013. Computer-Aided Design of Railroad Horizontal Arc Areas in Adapting to Satellite Measurements, *Journal of Transportation Engineering* 140(3). ID 04013017. http://dx.doi.org/10.1061/(ASCE)TE.1943-5436.0000643

Koc, W.; Palikowska, K. 2012. Dynamic Properties Evaluation of the Selected Methods of Joining Route Segments with Different Curvature, *Technika Transportu Szynowego* 9: 1785–1807 (Polish).

Koc, W.; Mieloszyk, E. 1998. Mathematical Modeling of Railway Track Geometrical Layouts, *Archives of Civil Engineering* 44(2): 183–198.

Li, X.; Li, M.; Wang, H.; Bu, J.; Chen, M. 2010. Simulation on Dynamic Behavior of Railway Transition Curves, *ICCTP 2010 Integrated Transportation Systems: Green, Intelligent, Reliable* 3349–3357. http://dx.doi.org/10.1061/41127(382)361

Long, X.; Wei, Q.; Zheng, F. 2010. Dynamic Analysis of Railway Transition Curves, in *Proc. of the Institution of Mechanical Engineers, Part F: Journal of Rail and Rapid Transit* 224(1): 1–14. http://dx.doi.org/10.1243/09544097JRRT287

Mieloszyk, E.; Koc, W. 1991. General Dynamic Method for Determining Transition Curve Equations, *Rail International - Schienen der Welt* 10: 32–40.

Tari, E. 2003. The New Generation Transition Curves, *ARI The Bulletin of the Istanbul Technical University* 54(1): 34–41.

Ziatdinov, R.; Yoshida, N.; Kim, T. 2012a. Analytic Parametric Equations of Log-Aesthetic Curves in Terms of Incomplete Gamma functions, *Computer Aided Geometric Design* 29(2): 129–140. http://dx.doi.org/10.1016/j.cagd.2011.11.003

Ziatdinov, R.; Yoshida N.; Kim, T. 2012b. Fitting G^2 Multispiral Transition Curve Joining Two Straight Lines, *Computer-Aided Design* 44(6): 591–596. http://dx.doi.org/10.1016/j.cad.2012.01.007

Received 14 February 2013; accepted 8 August 2013